



# Identity verification using palm print microscopic images based on median robust extended local binary pattern features and k-nearest neighbor classifier

Amjad Rehman<sup>1</sup>  | Majid Harouni<sup>2</sup>  | Negar Haghani Solati Karchegani<sup>3</sup> |  
Tanzila Saba<sup>1</sup>  | Saeed Ali Bahaj<sup>4</sup> | Sudipta Roy<sup>5</sup>

<sup>1</sup>Artificial Intelligence & Data Analytics Lab  
CCIS, Prince Sultan University, Riyadh, 11586,  
Saudi Arabia

<sup>2</sup>Department of Computer Engineering,  
Dolatabad Branch, Islamic Azad University,  
Isfahan, Iran

<sup>3</sup>Faculty of Computer Engineering, Najafabad  
Branch, Islamic Azad University, Isfahan, Iran

<sup>4</sup>MIS Department College of Business  
Administration, Prince Sattam bin Abdulaziz  
University, Al-Kharj, Saudi Arabia

<sup>5</sup>Artificial Intelligence & Data Science  
Programme, JIO Institute, Navi Mumbai,  
Maharashtra, India

## Correspondence

Majid Harouni, Department of Computer  
Engineering, Dolatabad Branch, Islamic Azad  
University, Isfahan, Iran.  
Email: m.harouni@iauda.ac.ir

## Funding information

No specific funding was received for this  
research.

**Review Editor:** Alberto Diaspro

## Abstract

Automatic identity verification is one of the most critical and research-demanding areas. One of the most effective and reliable identity verification methods is using unique human biological characteristics and biometrics. Among all types of biometrics, palm print is recognized as one of the most accurate and reliable identity verification methods. However, this biometrics domain also has several critical challenges: image rotation, image displacement, change in image scaling, presence of noise in the image due to devices, region of interest (ROI) detection, or user error. For this purpose, a new method of identity verification based on median robust extended local binary pattern (MRELBP) is introduced in this study. In this system, after normalizing the images and extracting the ROI from the microscopic input image, the images enter the feature extraction step with the MRELBP algorithm. Next, these features are reduced by the dimensionality reduction step, and finally, feature vectors are classified using the k-nearest neighbor classifier. The microscopic images used in this study were selected from IITD and CASIA data sets, and the identity verification rate for these two data sets without challenge was 97.2% and 96.6%, respectively. In addition, computed detection rates have been broadly stable against changes such as salt-and-pepper noise up to 0.16, rotation up to 5°, displacement up to 6 pixels, and scale change up to 94%.

## KEYWORDS

legal identity for all, local descriptors, median robust extended local binary pattern, microscopic palm print images, security

## 1 | BACKGROUND

Identifying individuals based on biometrics is one of the most urgent and vital issues in many areas, including security and surveillance (Saba, Haseeb, Ahmed, & Rehman, 2020). A wide range of individual identification systems need to be identified and verified (Raza et al., 2018; Rashid et al., 2020). For example, in security agencies, the office attendance device, ATMs, and even computer systems have been revealed the importance of identity verification more than

before. Biometric technology identifies people based on unique human characteristics such as the face, iris, vessels, and palm print (Fahad, Khan, Saba, Rehman, & Iqbal, 2018; Jamal, Hazim Alkawaz, Rehman, & Saba, 2017; Rahim, Rehman, Kurniawan, & Saba, ). In recent years, biometric technology with fingerprint features has been widely used. Still, for some reasons such as finger surface moisture, fingerprint degradation, and so on, it has always received severe criticism (Saba, Rehman, Altameem, & Uddin, 2014b). In addition, multiple biometrics such as fingerprints, faces and iris, palm vessels, and palm

print, have been introduced (Ahmad, Sulong, Rehman, Alkawaz, & Saba, 2014; Meethongjan, Dzulkifli, Rehman, Altameem, & Saba, 2013). Still, recent studies show that palm print, one of the best biometrics' features, can provide unique information about humans for machines identification (Khan, Javed, Sharif, Saba, & Rehman, 2019; Lung, Salam, Rehman, Rahim, & Saba, 2014). As with other biometrics, palm prints are unique, stable, and unchanged over time. Despite these advantages, palm print-based identity recognition systems still face a significant challenge called improper alignment, region of interest (ROI), in addition to noise-impacting images (Saba, Rehman, Altameem, & Uddin, 2014b; Iqbal et al., 2019; Joudaki et al., 2014). This may eventually lead to the loss of several pixels or alter some of the image information. This may also be due to human error, which is known as a common and inevitable challenge (Khan et al., 2021). Due to insufficient knowledge of how to use the system, when identifying, the users might put the hand on the scanner in a state other than the standard defined. This unavoidable error reduces the identification rate and disrupts the identification of some cases. Therefore, using a resistant method to this challenge seems to be an essential solution (Jabeen et al., 2018). Zhang, Wang, Huang, and Zhang (2018) presented a new method of identity verification by combining two features of weighted adaptive center symmetric local binary pattern (WACSLBP) and weighted Sparse Representation-Based Classification (WSRC). In their research, WACSLBP is used to extract important features such as image edges and major palm print. In this method, the CSLBP histogram is first removed from each sub-block, then if the subblock attribute information is high, the histogram will gain more weight and the subblock with less information will be assigned less weight. Finally, the produced histogram contains the most important information on the palm print image's edges, major lines, and wrinkles.

Finally, in this study, to reduce the computational complexity of the classification for the identification stage, the information differentiated between the test sample and each training sample using the Sparse Representation-based Classification weight structure of the WSRC algorithm is employed (Iftikhar, et al., 2017; Nodehi et al., 2014). The CASIA and PolyU data sets were used to evaluate the proposed method and the test images were identified in ten inappropriate image modes (CASIA Dataset). At the end of the study, a 98% identity verification rate was reported, which is considered acceptable about the challenges of the rate test images. Nonetheless, this research could have been more comprehensive by applying important challenges such as displacement, rotation and scale of research.

Rida, Herault, Marcialis, and Gasso (2019) examined the impact of using ensemble classification based on data-driven features in their research. The purpose of this study was to present a method of group classification using the Random Subspace Method. This method relies on the two-dimensional principal component analysis (2DPCA) non-random technique and provides approximately distinct random subsets. Thus, after calculating the data variance in two-dimensional space, the first components are considered the strongest image information and generated a subset of data. At this point, the attributes of each subdomain are extracted using two-dimensional linear discriminant analysis (2DLDA). Then, in the classification section using a – 1

class the nearest neighborhood of these subsets is classified. At the end, the identification is carried on using an identification method of voting. The data used in this study were selected from the PolyU data set, and the method presented on these images was evaluated in red, green, blue, infrared, colored, and 2D bands. The results of this evaluation of the test images show that in all of the mentioned challenges except the 2D images, the detection accuracy was higher than 99%. In the 2D images challenges, the test images were identified with 94% accuracy. According to the obtained results, this is qualitative research, although the method is very fast in terms of time complexity, but the challenges posed in this research are far from the challenges in reality and therefore cannot be investigated, and from this perspective, it cannot be known as comprehensive research.

Almaghtuf and Khelifi (2018) presented a method based on the self-geometric relationship filter to improve the fit of points selected by the scale-invariant feature transform (SIFT) algorithm. In this study, due to the weakness of the SIFT algorithm in point matching, a geometric filter to establish relationships between selected points and compare the geometric patterns for identification has been used. In the preprocessing section of the ROI, the full image is extracted. The study is performed on the PolyU II data sets. Then, the images of the other two data sets are presented as ROIs. Finally, the SIFT algorithm is applied to the ROI from palm print images to extract key features in the next step. However, their approach is based on Euclidean distance that could not meet the challenges of this field.

For this reason, a central point filtering method is introduced in response to this challenge. So that after selecting several points as the central point at defined angles, the nearest points to the central point are identified and connected to the central point. Multiple graphs are created for each image, and finally, they will identify the central points with regard to the points connected to them. Evaluation of this method was carried out using three data sets IIT-Delhi, PolyU, and THUPALMLAB. Their study might not be comprehensive despite the good results since it has not addressed rotation, displacement, or image scaling issues. El-Tarhouni, Boubchir, Elbendak, and Bouridane (2019) presented an approach based on pyramid histogram orientation gradient and Pascal coefficients of local binary patterns to improve the identity verification rate using palm print images. Their research is composed of a few stages. In the first stage, only the Pascal Coefficient Multiscale Local Binary Pattern (PCMLBP) descriptor was used to extract the features to compare the primary method of this study. Secondly, Pyramid Histogram Orientation Gradient descriptor has been used along with PCMLBP. Using this descriptor makes the proposed method resistant to light changes. Thirdly, PCA is used to reduce the dimensionality of the feature vectors and finally the random subspace LDA is used for classification.

The classification methods could be divided into two categories; first, calculating the confidence values for each class, and second, determining the class indicator whose test sample has reached the maximum score in relation to the class (Rehman et al., 2021; Khan et al., 2020). The image data set used in this study is PolyU, and the images are analyzed in four red, green, blue, and infrared bands. Also, the detection rate in the proposed method is over 99% across all four bands. But what distinguishes this research from comprehensive

research is that it does not evaluate any significant challenges and is far from a real-world implementable system (Saba, 2020). Minaee and Wang (2016) used a convolutional neural network and developed a new way of identity verification. This research has tried to improve the identity verification rate in palm print images by deep learning.

In the same way, after preprocessing the images, the feature of the images is extracted using a scatter wavelet. The important thing about using this descriptor is that it first has a lot of parameters that include the degree, direction, and depth of the wavelet. The degree and direction of the filters used in the algorithm were a very large set of Gabor Violet filters. The wavelength was related to the dispersion of the algorithm used in the proposed method. The first depth for this algorithm worked much like the SIFT algorithm, and the second depth acted like the directed sphere exclusion algorithm. Since the more algorithms operated in their research, the larger and distinctive feature vectors were produced, so the algorithm's time complexity increased. Finally, after a subsequent reduction step by PCA using SVM classification, all the feature vectors had been classified and identity verification had been obtained. This method has been evaluated using PolyU data set images, and a 100% recognition rate has been claimed. However, although this method has the highest possibility of identification, no major challenge has been addressed in this study to test the robustness of the approach against changes.

Fei et al. (2017) proposed a method based on local binary patterns for identity verification with palm print imagery. They tried to improve the algorithm detection of local binary patterns. In this study, a local orientation binary model (LOBP) is introduced, in which Orientation Binary Pattern (OBP) and Confidence Binary Pattern (CBP) statistical blocks are used to create a global high-speed descriptor. In their method, the image is first divided into  $16 \times 16$  nonoverlapping blocks. The principal orientation, corresponding values, and confidence are extracted for each block to obtain the OBP and CBP maps. The OBP and CBP histograms are then calculated. The OBP and CBP histograms are merged to create a global histogram, and the final feature vector is created. Finally, by adopting the distance calculation system, identification is made. For evaluating the proposed method, three data sets of PolyU, M Green, and IITD were used. The results show that the proposed method outperforms the methods being assessed and has been able to calculate the identity verification at 100%. However, this study has addressed no significant challenges, which indicates that the study is incomplete. Mokni, Drira, and Kherallah (2017) used contexture and geometric properties in their study for calculating identity verification. This study presents a new method for extracting major palm prints and a new geometric structure to analyze geometric shapes. In the geometric properties section, the major palm print lines are extracted using three types of curves: steerable and hysteresis filters. Then new curve lines are generated by averaging operations of the curves. In the contexture properties section, palm print image features are extracted using fractal analysis and calculating fractal dimensions. The extracted features are merged at the end of this section to improve identification accuracy in geometric and contexture sections. At the end of this study, the data are categorized by random forest based on geometrical, contexture, and merged features, and the identification rate of each segment is calculated

separately. Three data sets of PolyU, CASIA, and IIT-Delhi were used to evaluate the proposed method. The evaluation results show that the identification rate with geometric properties is 93%, the contexture features 96%, and the integration of the two features 98%. Although this study yields acceptable results and confirms the effect of integrating the results of different descriptors, it has not been evaluated in challenges such as rotation, transfer, and scale, which could be a flaw for this research (Saba et al., 2014b).

Tamrakar and Khanna (2016) used a Resource Description Framework (RDF) descriptor to investigate the identity verification of palm print images in their study to provide a stable rotation and noise method. The study used three data sets that extract the ROI of two data sets from the image, which means that this study involves a preprocessing step. In the feature extraction step, RDF descriptor is used based on radon, dual-tree complex wavelets, Fourier transforms. The integration of the properties of these three descriptors strengthens the proposed method against rotation and noise. A dual-tree complex wavelet is applied to the radon extraction angle in a multi-resolution path since radon coefficients contain contexture information from the image and after calculating the radon coefficients. Then, high-frequency coefficients are extracted to extract the feature. Finally, applying the instant two-dimensional conversion eliminates circular transmission. Lastly, it should be noted that this method is very stable compared to the conditions mentioned above.

In the end, the vectors are classified by the nearest neighborhood cluster. The data used to evaluate this study are from the three data sets PolyU, CASIA, and IIT-Delhi, and the results show that the proposed method is relatively stable to rotation and noise. Still, fundamental challenges such as transitions and scales are not investigated in the above study. Xu, Fei, and Zhang (2014) combined a fascinating study of left and right palm print images to improve the identity verification rate. This research has been implemented in three different phases. The first two phases are about identity verification using left- and right-hand images. The third phase is about identity verification by combining the two hand identifications. Lastly, the final decision phase of this research is about integrating left- and right-hand results, and both hands are at the level of decision. In the preprocessing stage, only the ROI of the hand is removed from the image. The extracted features of this study are very comprehensive and use a wide range of descriptors, including Gabor filter, Sparse Multiscale Competitive Code (SMCC), derivatives of Gaussians, and Sparse Multiscale Competitive Code, and are adapting SIFT, PCA, LDA, 2DLDA, and 2DPCA algorithms.

Collaborative Representation-based Classification and Two-Phase Test Sample Sparse Representation have been used, which can be unreliable and have compared several categories to identify the best method. The images used to evaluate the proposed method are from both PolyU and IITD data sets, and the results show that the proposed method has a very appropriate identification rate, but the only point that can be considered as a flaw for this realization is the lack of investigation of the proposed method with significant challenges such as noise, rotation, and scale is observed on images. As mentioned before, most of the research is implemented in a common format and only performs the identification process in the most ideal way. But

the world of reality is the world of error such as error in identifying palm print, error in scanner, and malfunction. The existence of such errors indicates the need to implement methods concerning such errors. For example, an error in correctly identifying the ROI region by the segmentation algorithm can result in the image generated from the ROI region relative to the target image, with some rotation, transfer, scale resizing, and so on (Khan et al., 2021).

On the other hand, the scanner has a technical problem and the scanned images are noisy (Saba, Rehman, Al-Dhelaan, Al-Rodhaan, 2014). If all of the above are put together by human errors in using security systems, what is certain is that the real situation is by no means the ideal one (Sharif et al., 2019). This article's main purpose is to define several unavoidable challenges in real systems to investigate the robustness of the method presented in this study against these changes. These challenges include noise, scale change, transmission, and rotation. Figure 1 illustrates an example of these challenges.

As shown in Figure 1, there are two types of changes in the image. The first change is in the pixel brightness values, that is, by rotating, moving, and resizing all pixel values and by applying a large portion of the pixel brightness values. The second change is the loss of a portion of the image lost by the challenge of transmitting a portion of the pixels of the image border. Therefore, the purpose of this study is to present a method that can generate distinct feature vectors despite overall changes in the image to classify the images into correct classes. For this purpose, in this study, we use median robust extended local binary pattern (MRELBP; Liu

et al., 2016) to extract features from images. Instead of extracting attributes from pixel values, this method uses a neighborhood area to generate the attribute of each pixel. This causes changes in pixel values to produce less change in the output of image feature vectors, and the feature vectors have the required stability against changes.

This research is further composed of four main sections. In Section 2, the MRELBP algorithm is presented, and Section 3 presents proposed method in detail. Section 4 exhibits results and discussion, and finally, Section 5 concludes the research.

## 2 | THE MRELBP ALGORITHM

The RELBP algorithm is of three GRELBP, ARELBP, and MRELBP families (Liu et al., 2016). The difference among these three algorithms is the type of filter used. If the GOSIN filter is used in the RELBP algorithm, this is called the GRELBP algorithm. If the average filter is used in the RELBP algorithm, this is called ARELBP algorithm, and if the median filter is used in this algorithm, the generated algorithm is called MRELBP. The RELBP algorithm behaves very similar to ELBP and consists of three descriptors RELBP\_CI, RELBP\_NI, and RELBP\_RD. The only difference with ELBP is that instead of using a pixel in the computation, it uses a block for analysis and for having a value of one particular unit of block, it uses three filters, namely, GOSIN, mean, and median which are listed. This section will provide a detailed description of this algorithm.

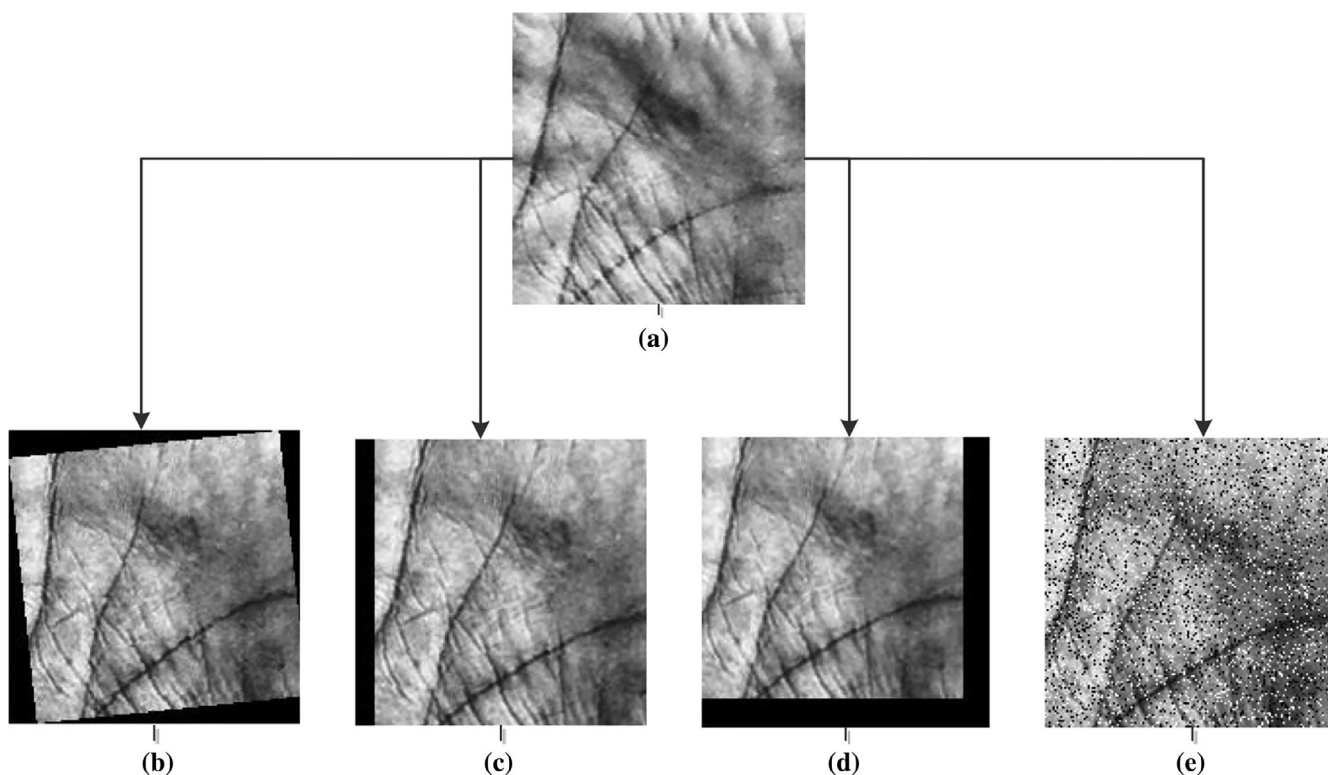


**FIGURE 1** (a) Image without challenge, (b) image with rotation challenge, (c) transition challenge image, (d) image with scale change challenge, and (e) noise challenge image

## 2.1 | RELBP\_CI descriptor

This descriptor is calculated by Equations (1) and (2).

$$\text{RELBP\_CI}(x_c) = s(\phi(X_{c,\omega}) - \mu_\omega), \quad (1)$$

$$\mu_3 = \frac{1}{N} \sum_{c=0}^N \phi(X_{c,\omega}). \quad (2)$$

Figure 2 shows the block in which the central pixel is located and is shown in gray in this Figure. Also, in Equation (2),  $\mu_3$  represents the average brightness of the block ( $X_{c,\omega}$ ) and  $\phi(X_{c,\omega})$  applying one of the filters to the block ( $X_{c,3}$ ). The function  $S$  compares the desired block with the specified threshold, such that if the value inside this function is less than zero, the result of the whole function becomes zero, and if the value inside this function is higher than zero, the result of the whole function is 1 and multiplied in  $2^n$ . So,  $\text{RELBP\_CI}(x_c)$  for each block can have only two values 0 or 1.

## 2.2 | RELBP\_NI descriptor

This descriptor is calculated by Equations (2) and (3).

$$\text{RELBP\_NI}_{r,p}(x_c) = \sum_{n=0}^{p-1} s(\phi(X_{r,p,\omega_r,n}) - \mu_{r,p,\omega_r}) 2^n, \quad (3)$$

$$\mu_{r,p,\omega_r} = \frac{1}{p} \sum_{n=0}^{p-1} \phi(X_{r,p,\omega_r,n}). \quad (4)$$

In Equations (3) and (4),  $r$  represents the neighborhood radius and  $p$  the number of neighborhood blocks with the radius and dimensions of the neighborhood block. Regarding identifying neighboring blocks, these blocks are at angles similar to the ELBP method with centering the ( $X_{c,\omega}$ ) and radius  $r$  located in the  $2\pi/p$  aspects. Figure 2 shows the location of adjacent blocks. For example, and a summary for this section, it should be noted that according to Figure 5, RELBP\_NI for a radius  $r_2$  equal to the LBP algorithm is applied to the median (and also mean or Gaussian filter) of the blue blocks and are considered as threshold values of the mean of the median of the blue blocks.

## 2.3 | ELBP\_RD descriptor

This descriptor is calculated using Equation (5).

$$\text{RELBP\_RD}_{r,r-1,p,\omega_r,\omega_{r-1}}(x_c) = \sum_{n=0}^{p-1} s(\phi(X_{r,p,\omega_r,n}) - \phi(X_{r-1,p,\omega_{r-1},n})) 2^n. \quad (5)$$

As shown in Figure 3, the radial difference in the radius  $r$ ,  $r-1$ , and the number of  $p$  blocks are equal to the LBP algorithm applied

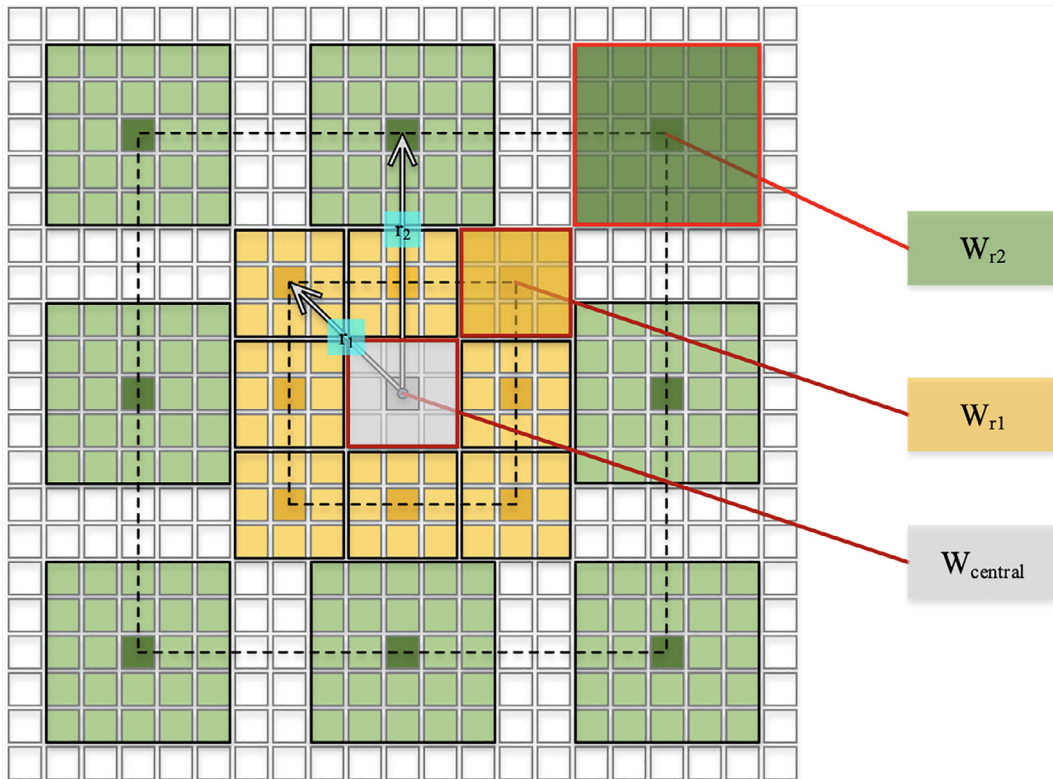
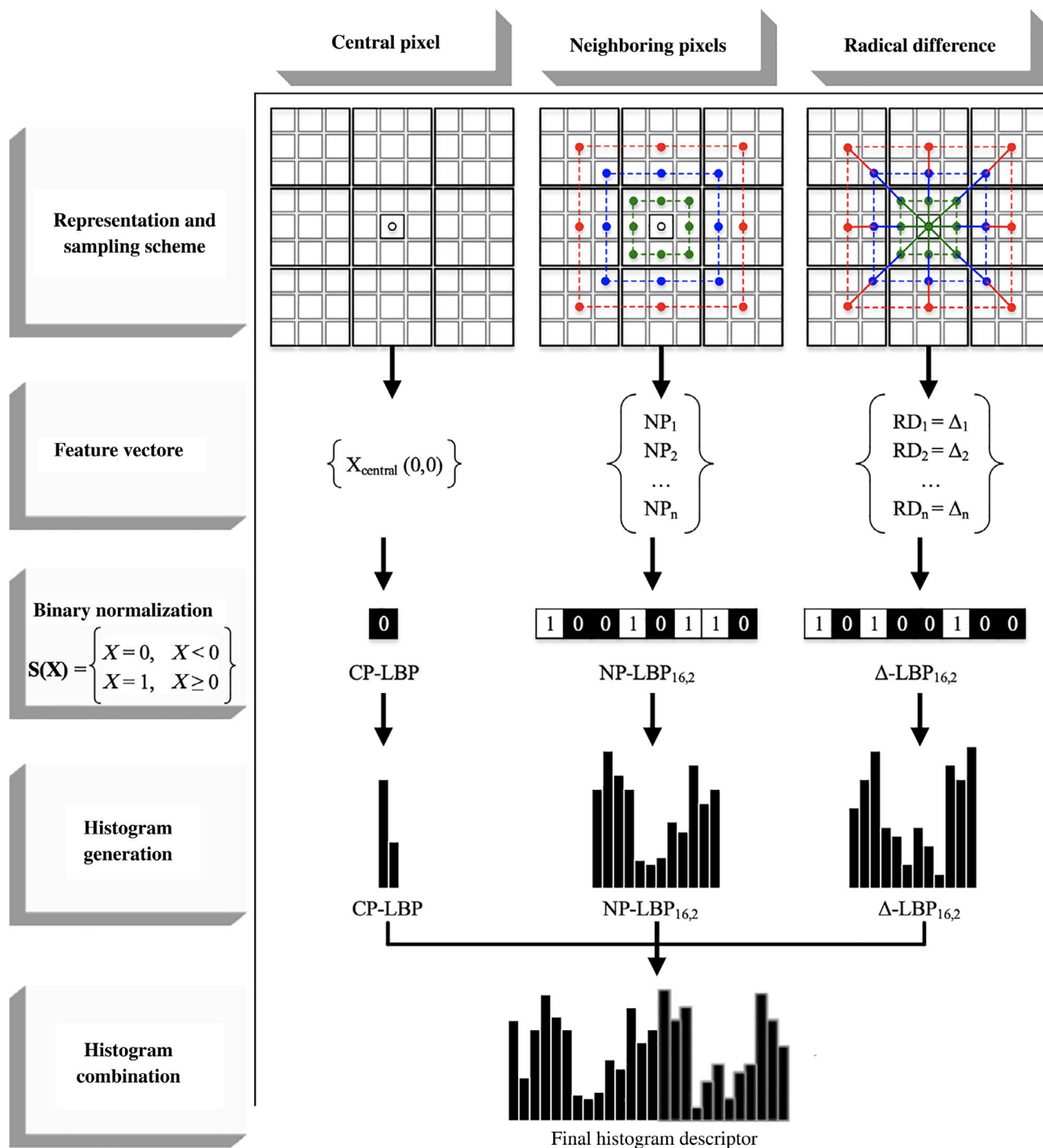


FIGURE 2 Algorithm works RELBP





**FIGURE 3** Results integration of three descriptors. CP, Central pixel; LBP, Local binary pattern; NP, Neighboring pixels; RD, Radical difference

to the filtered radius  $r$  blocks which are equal to the threshold of the filtered blocks  $r - 1$ . Figure 3 shows how this descriptor is calculated. For example, the middle of the red block is reduced to the middle of the blue block and the LBP algorithm is applied to it. All three categories of attributes are derived from the descriptors described in the LBP codes. Therefore, it is possible to integrate these features to produce more distinctive feature vectors (Liu, Zhao, Long, Kuang, & Fieguth, 2012). The histogram is produced by integrating the three descriptors RELBP\_CI, RELBP\_NI, and

RELBP\_RD as the final image histogram is generated in the last step. Figure 3 illustrates how to integrate the properties of these three descriptors.

### 2.4 | Features extraction process

The features extraction methods reported in Section 1 are calculated on a radial difference layer and a neighborhood layer.

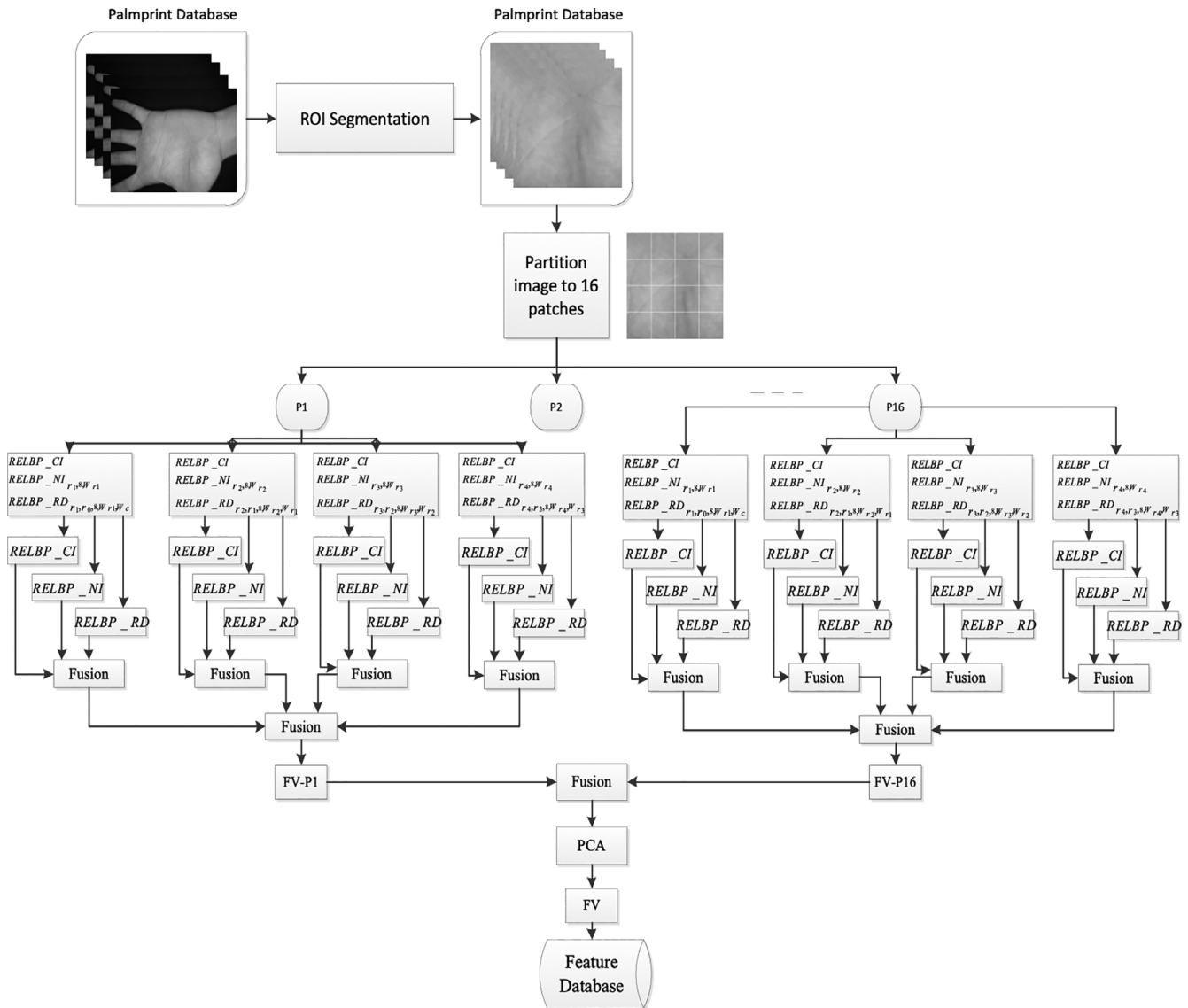


**FIGURE 4** Integrating the RELBP algorithm into four layers. CI, Central intensity; NI, Neighboring intensities; RD, Radial difference; RELBP, Robust extended local binary pattern

However, this study used four layers of neighbor and radial divergence to extract the feature from the image(s) and apply filters on the blocks using a median filter. Finally, the histograms generated from each layer are generated by combining the histograms RELBP\_CI, RELBP\_NI, and RELBP\_RD and merging and producing the final image feature vector. Figure 4 shows an overview of the method of Liu et al. (2012).

### 3 | PROPOSED METHOD

The identity verification system introduced in this research is based on a local feature extractor and a supervised classification. Like many similar systems, the system consists of four stages: palm print segmentation, feature extraction, feature selection, and classification. Figure 5 shows the proposed method in the training phase.

#### 3.1 | Palm print area segmentation

In this study, images of two data sets (Kumar, 2008; Kumar & Shekhar, 2010) IITD and CASIA (“CASIA data set”) were used. The IITD data set images are provided as ROIs, and the images in this data set do not need to be segmented. Still, the CASIA data set images are raw and without any preprocessing, so processing the images in this data set data requires a segmentation and ROI extraction step. Therefore, Zhang et al.’s (2018) method is used to localize the images in this data set. Figure 6 shows a sample of CASIA data set images before and after segmentation.

#### 3.2 | Features extraction

Unique features extraction is a critical stage in the whole process of identity verification (Jadooki, Mohamad, Saba, Almazayad, &

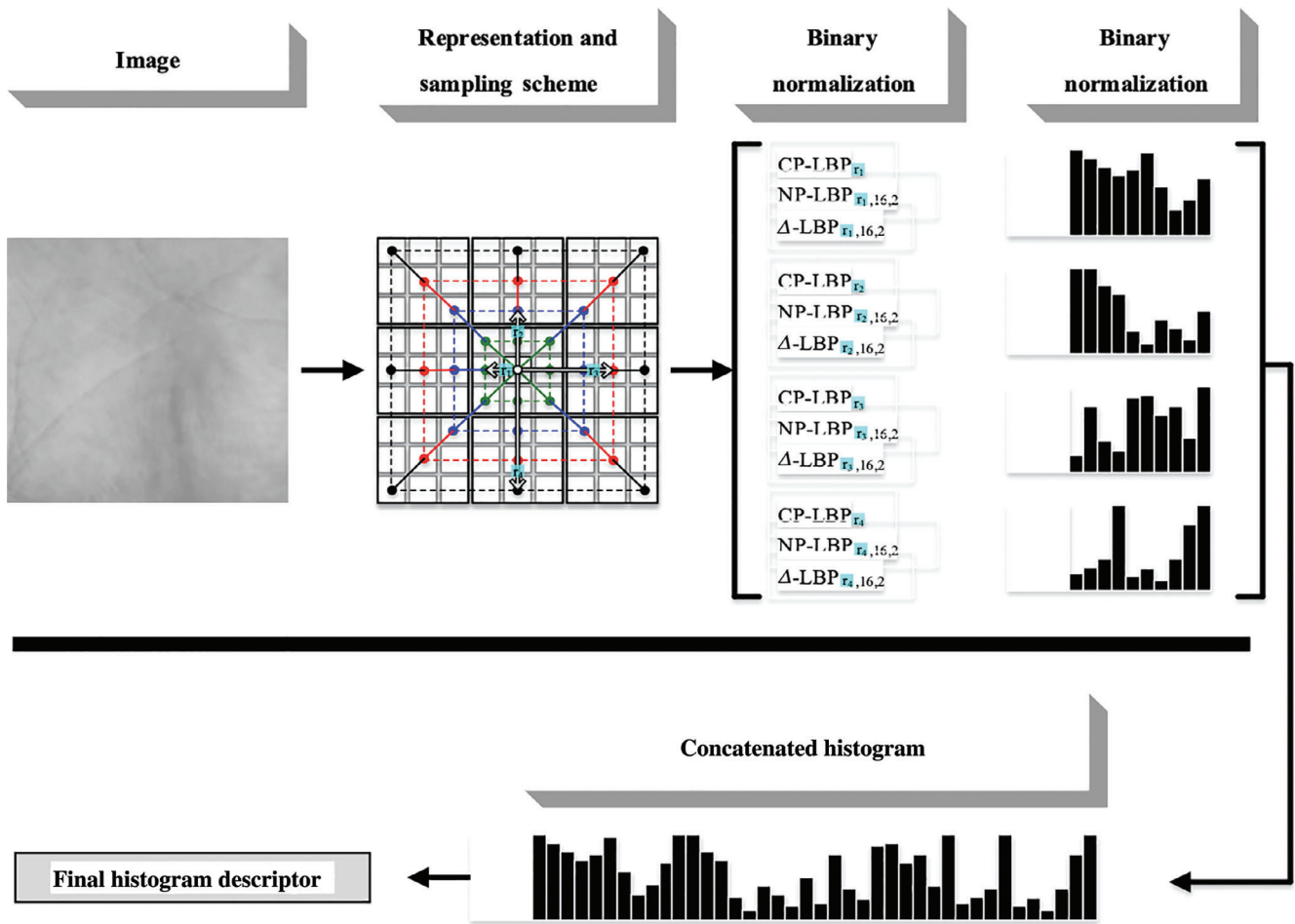


**FIGURE 5** Proposed method in the training phase. CP, Central pixel; LBP, Local binary pattern; NP, Neighboring pixels; RD, Radial difference

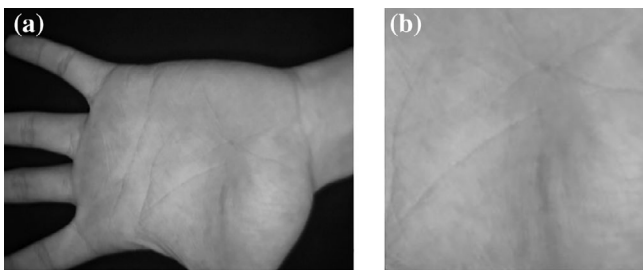


**FIGURE 6** CASIA data set microscopic images: (a) before fragmentation and (b) after segmenting and extracting the ROI area. ROI, Region of interest

Rehman, 2017; Yousuf, Mehmood, Habib, et al., 2018). In the identification process, feature extraction is one of the most sensitive and challenging stages of research (Mittal et al., 2020; Saba, 2019; Saba, Almazyad, & Rehman, ).

As mentioned in Subsection 2.4, generalized sustainable binary patterns (MRELBP) were employed to extract the features. First, the nonoverlapping images are divided into 16 blocks completely equal. Then, the properties of RELBP\_CI, RELBP\_NI, and RELBP\_RD are

extracted following Figure 4 for the pixels of each block in four layers, and according to Figure 5, the features extracted by these three descriptors are merged into the four layers described in Section 2. This step is repeated for all 16 blocks, and finally, the property of the 16 blocks is combined and the image property vector is generated.

### 3.3 | Features selection

Features selection is the process of selecting the most discriminative features from selected features that could identify the object uniquely (Sharif et al., 2019; Amin, Sharif, Raza, Saba, & Anjum, 2019). Scene analysis and search using local features and support vector machine for effective content-based image retrieval. Since the MRELBP descriptor extracts image properties in multiple layers and internal descriptors, generating a large volume of features for each image is very natural (S. A. Khan, Nazir, et al., 2019). But it should be borne in mind that many of the features produced do not contain useful and distinctive information about the image (Harouni et al., 2014; Neamah, Mohamad, Saba, & Rehman, 2014). Therefore, after extracting the feature from the images, an essential feature selection



algorithm is performed on the generated feature vectors using the PCA algorithm to reduce feature-length vectors and reduce computational and temporal complexity in the classification stage. Another important point to note about PCA is that it eliminates the correlation between attributes and enhances the differentiation of attribute vectors of different classes, which ultimately improves the identification rate (Rehman et al., 2020; Rehman, Alqahtani, Altameem, & Saba, 2014).

### 3.4 | Classification

Following the production and improvement of feature images vectors of training, it is time to identify the test feature vectors (Ramzan et al., 2020). Figure 7 shows the block diagram of the classification of test images.

The main purpose of this research is to identify individuals with altered or damaged palm print images. In a clear sense, the images in the training phase are without any challenges. Still, the identity of these images or individuals must be tested with images that do not meet the ideal conditions for training images. Thus, as shown in Figure 7, the performance and efficiency of the proposed method are tested with images subjected to challenges such as noise, scale change, rotation, and transfer. In the remainder of this study, and in

Section 4, results of the proposed method's robustness against these challenges are presented.

## 4 | EXPERIMENTAL RESULTS

In this section, the efficiency of the proposed method is evaluated using CASIA and IITD data set images since the proposed method in this study contains many parameters in the feature extraction and classification section. First, the method parameters are described in Table 1; this table provides a complete description of the three methods compared. These parameters will be constant at all stages of the test.

In the following section, we first describe the images data set used in experiments, results, and comparisons of proposed approach in state of art.

### 4.1 | Data sets

Benchmark data sets play an important role in evaluating the reported techniques and their results comparison in state of the art (Rehman et al., 2018; Rehman & Saba, 2011). Therefore, microscopic palm print images of both IITD and CASIA data sets were used to evaluate the

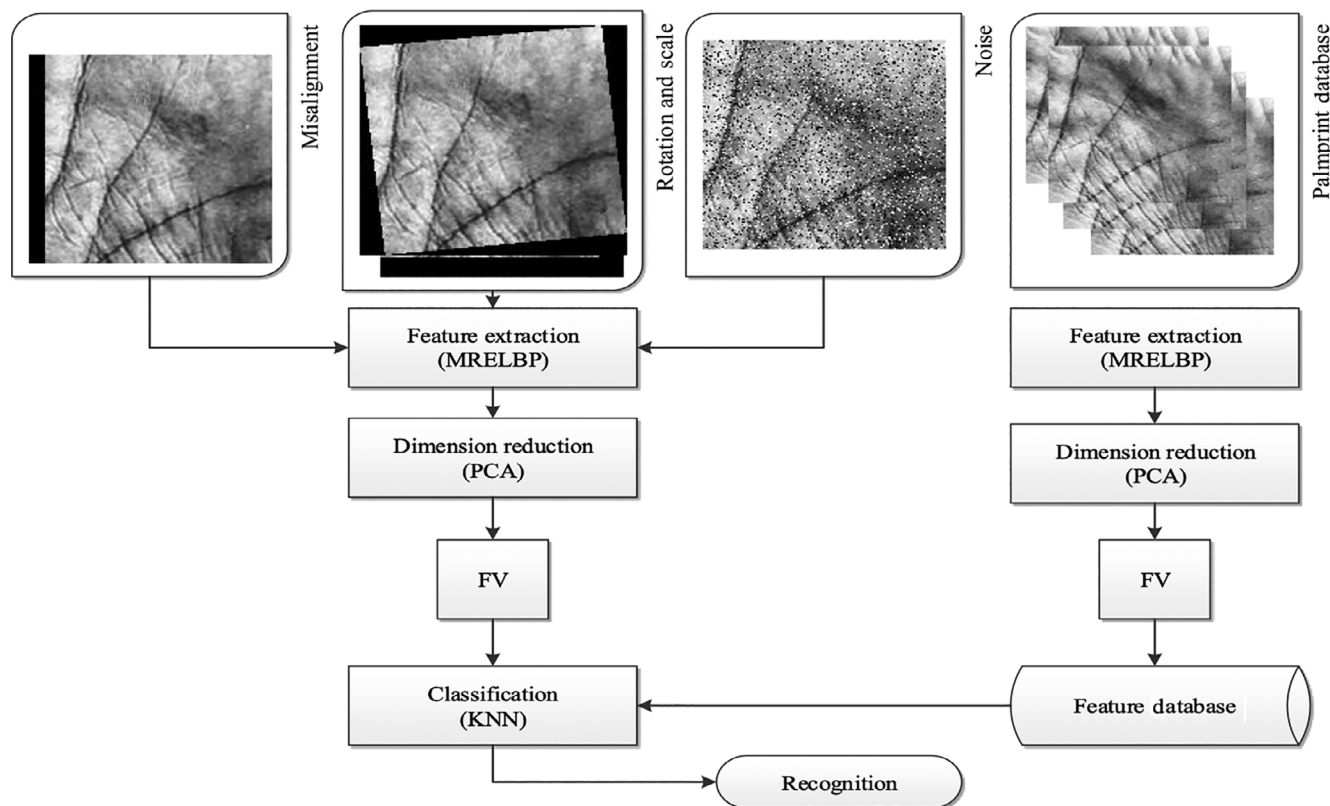


**FIGURE 7** Block diagram of the classification of the test images. KNN, K-nearest neighbor; MRELBP, median robust extended local binary pattern; PCA, principal component analysis

**TABLE 1** Parameters' description in the methods

Method	Specification
Proposed method	<ul style="list-style-type: none"> <li>• Neighborhoods used to extract the properties of each pixel are four neighbors.</li> <li>• The filter used in the RELBP algorithm is the middle filter, so the method used is MRELBP.</li> <li>• Neighborhood radii in the proposed method are 2, 4, 6, and 8.</li> <li>• There are eight blocks in each neighborhood area, so the center of the blocks is 45° from each other relative to the central block.</li> <li>• Neighborhood blocks are 2 pixels in diameter and the remaining neighbors are 5 pixels.</li> <li>• The neighborhood radius of the KNN class is <math>K = 1</math>.</li> <li>• In the noise challenge of this study, salt-and-pepper noise test images were applied in the range from 0 to 0.32.</li> <li>• In the rotation challenge of this study, the test images were evaluated in the range from 0 to 6°.</li> <li>• To the detriment of this research criticism, the test images move in the positive direction of the x axis between 0 and 12 pixels.</li> <li>• In the scale challenge of this study, the test images will have a scale change from 0 to 12.</li> </ul>

Abbreviations: KNN, K-nearest neighbor; MRELBP, median robust extended local binary pattern.

**TABLE 2** Specifications of the databases

	Database	
	IITD database	CASIA database
No. of subjects	235	312
Number of still images per subject (two hand)	14	More than 20 samples
Distance	Variable	Stable
Resolution	800 × 600	640 × 480
ROI resolution	150 × 150	200 × 200
Format	.bmp	.JPG

Abbreviation: ROI, Region of interest.

proposed method. Accordingly, the images of these two data sets are divided into three sections. The first section contains images that identify the best parameters in the proposed method descriptor and classifier. The second part consists of instructional images that comprise 40% of the data set images, and the third is the images that the proposed method is tested with. Table 2 shows the specifications of both data sets.

## 4.2 | Test implementation hardware and software platform

MATLAB R2017a simulates the proposed method on Windows 10 operating system, and the hardware platform used to simulate this

research is an Intel® Core™ i5-8500 system with 8 GB of RAM, plus 16 GB of RAM from the SSD hard drive.

## 4.3 | Analysis and discussion

A few essential points should be noted in detail for the implementation of the proposed methods and the methods being evaluated. First, a sampling of training and test images was random in all experiments. Five images were selected from six images per hand for training. One image was rotated, transposed, scaled, and applied noise to the image and was randomly selected for the test. In the method proposed in this paper, the set of images used in the experiments to identify the best parameters is removed from the set of images of the original experiments. The data sets used in these experiments for both data sets were 600 images of 100 individuals (five images were taken from each person for training and one image for the test). Then, the introduced and compared method was repeated 10 times with random sampling for the test and training set and recorded for each run of identification accuracy. The accuracy of the identification recorded in the results table is 10 times the average of these tests as well as taking into account the accuracy of identifying 10 times each test and the 95% confidence interval of the confidence interval range of all experiments (Saba et al., 2018). Tables 3–6 show the results of this study.

Table 3 presents the results of image identification rates under the influence of salt pepper noise in the range from 0 to 0.32. As can be deduced from the results of this challenge, the detection rate is not significantly affected by salt pepper noise, and when the noise exceeds the range of 0.16, the detection rate decrease is more noticeable. But consider Figure 2 to better understand the cause of this persistence. It can be seen in this figure that first for a pixel, several properties of neighboring radii are extracted; secondly, in each radius, eight blocks are used to extract the properties, and thirdly, each block is used as a threshold value for computation. The use of a middle filter essentially makes any method resistant to noise (Saba et al., 2014a). In addition, feature extraction from a relatively large area causes partial damage to the area to have little effect on the quality of the properties extracted from the entire area. Figure 8 compares the identification rates of the two data sets used in this study under noise challenge.

Table 4 presents the results of the identification challenge with the rotation challenge between 0 and 6°. As it can be seen, the proposed method still has a relatively stable rotation. But the reason for this stability is that the feature is extracted for a pixel in the four circles. Thus, to some extent, the rotation of the image only causes the selected block areas to change slightly, which cannot significantly impact the detection rate. Figure 9 compares the identification rates of the two data sets used in this study under the influence of the rotation challenge.

In Table 5, the proposed method results are compared with the challenge of transmitting image pixels in the range from 0 to 12 pixels in the x axis direction. The values obtained by calculating the

**TABLE 3** Identification results of the salt-and-pepper noise challenge

	Noise level					
	0	0.02	0.04	0.08	0.16	0.32
Average IITD	97.2	97.45	97.55	97.20	96.85	87.65
IITD confidence interval	96.56–97.83	96.87–98.11	96.75–98.34	96.74–97.65	96.02–97.67	85.86–89.43
CASIA average	96.60	94.15	92.22	90.10	86.85	81.20
CASIA confidence interval	95.87–97.33	93.30–95.00	91.24–93.20	89.18–91.02	85.75–87.95	79.63–82.77

**TABLE 4** Results of the spin challenge identification

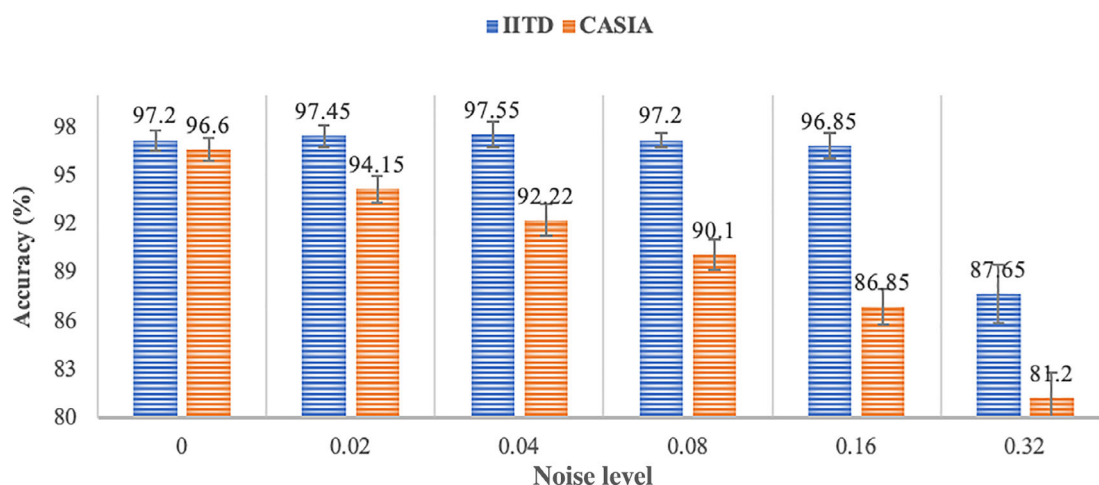
	Rotation rate					
	0	2	3	4	5	6
Average IITD	97.2	96.85	95.50	94.10	91.65	87.55
IITD confidence interval	97.83–96.56	97.50–96.19	96.48–94.51	94.93–93.26	93.04–90.25	89.36–85.73
CASIA average	96.60	95.96	93.70	92.20	89.11	86.15
CASIA confidence interval	95.87–97.33	95.15–96.77	92.75–94.65	91.16–93.24	88.03–90.19	84.80–87.50

**TABLE 5** Results of transition identification challenge

	Transfer rate					
	0	1	3	6	9	12
Average IITD	97.2	96.90	96.55	95.70	90.70	82
IITD confidence interval	96.56–97.83	96.21–97.60	95.80–97.29	94.65–96.74	89.68–91.71	80.78–83.21
CASIA average	96.60	96.45	95.22	94.84	91.36	85.20
CASIA confidence interval	95.87–97.33	95.59–97.31	94.32–96.12	93.85–95.83	90.30–92.42	83.99–86.41

**TABLE 6** Results of scale challenge identification

	Scale rate					
	0	2	3	6	9	12
Average IITD	97.2	97.45	96.95	94.25	86.10	54.25
IITD confidence interval	96.56–97.83	96.87–98.02	96.13–97.76	93.51–94.98	84.34–87.85	43.08–65.41
CASIA average	96.60	96.22	96.39	95.02	90.77	68.56
CASIA confidence interval	95.87–97.33	95.41–97.03	95.46–97.32	94.12–95.92	89.60–91.94	66.96–70.16

**FIGURE 8** Comparison of IITD and CASIA data set identification rate comparison under noise challenge

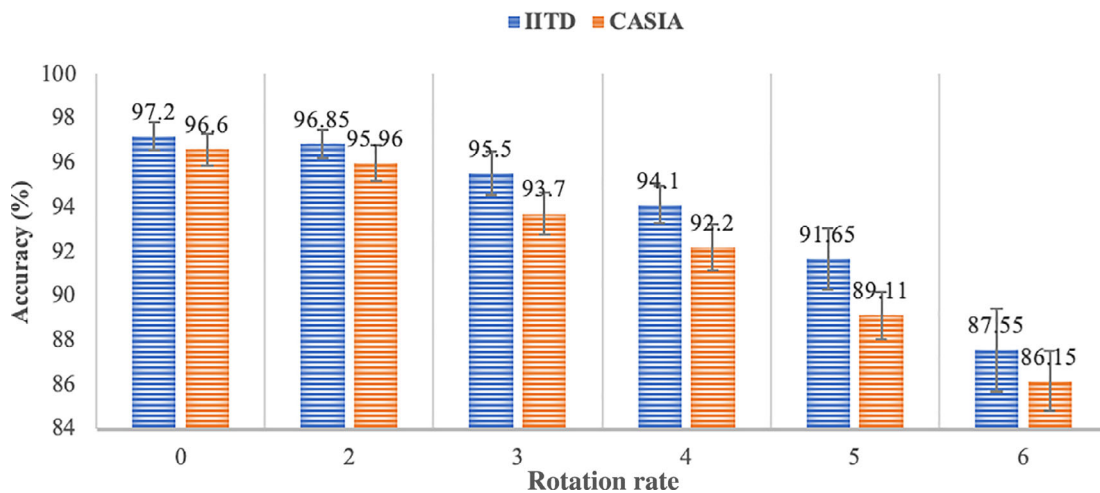


FIGURE 9 Comparison of IITD and CASIA data set identification rates under the rotation challenge

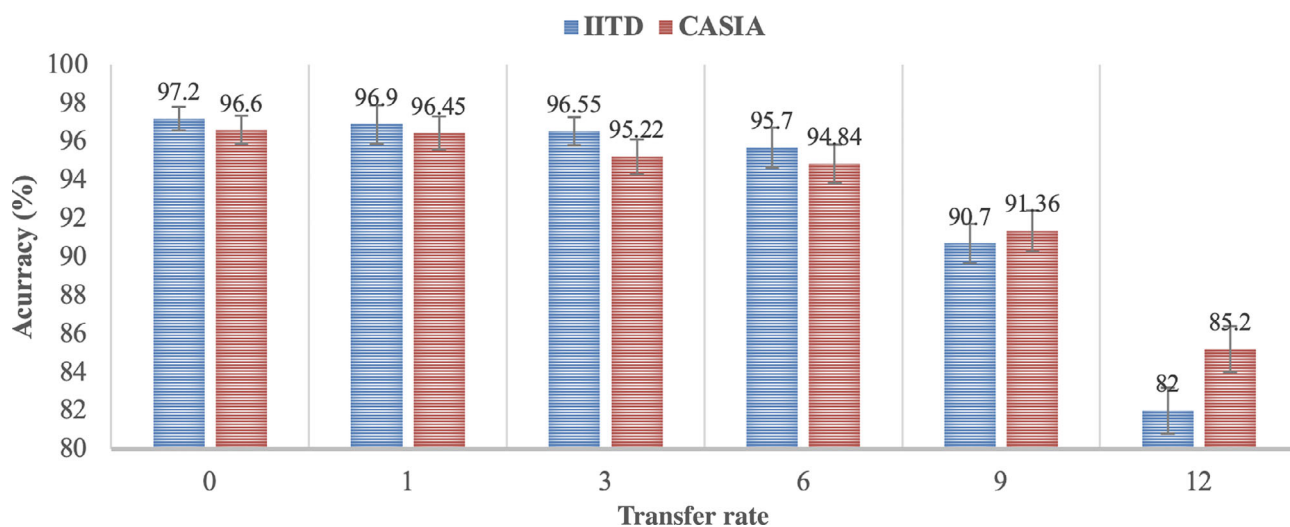


FIGURE 10 Comparison of IITD and CASIA data set identification rate under transition challenge

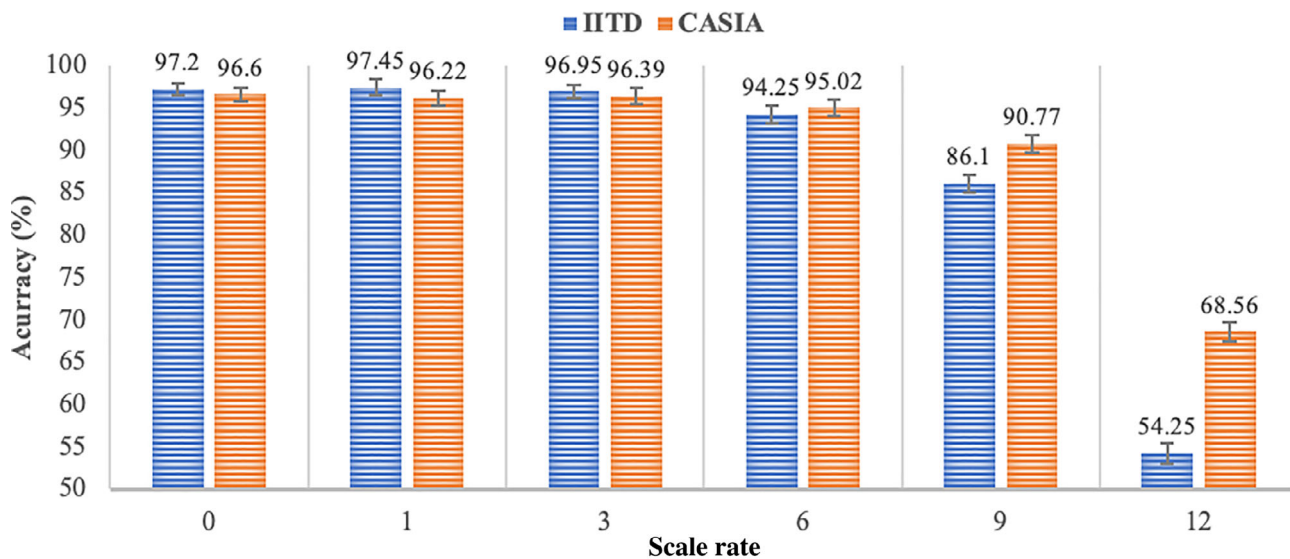


FIGURE 11 Comparison of IITD and CASIA data set identification rates under scale challenge

detection rate of the proposed method in this challenge also indicate the stability of the proposed method against image transfer. It can be said that the stability of the proposed method is that only part of the image margin is separated from the original image and the proposed method extracts the necessary and distinctive attributes for each class image from the remainder. Figure 10 compares the IITD and CASIA data set identification rates under the transition challenge.

At the end of this section, the scale challenge results are presented in Table 6. This challenge shrinks the image of many of the tissues in the image. But the proposed method still produces the remaining texture vectors for each class with precise and distinctive features, thus preventing a noticeable reduction in the identification rate in the image. Figure 11 compares the IITD and CASIA data sets identification rates under the scale challenge.

## 5 | CONCLUSION

In this paper, a new method for identity verification based on palm print microscopic images is presented. In the proposed method, four critical identity verification challenges were investigated by image angular modification, image transfer, image scaling, and noise. A local descriptor was used as MRELB. Extracting features from a large area around the pixels makes the method very stable against many issues, including the earlier challenges. Following features extraction, the PCA is used to reduce the dimension and the correlation of the feature vectors, all of which ultimately led to the proposed system's stability against changes. Finally, k-nearest neighbor classifier attained state-of-the-art 97.2% and 96.6% identity verification accuracy without challenges on two benchmark data sets IITD and CASIA, respectively.

### ACKNOWLEDGMENT

This research is technically supported by Artificial Intelligence and Data Analytics Research Lab (AIDA) CCIS Prince Sultan University, Riyadh, Saudi Arabia. The authors are thankful for this support.

### CONFLICT OF INTEREST

The authors declare no conflict of interest and all authors contributed equally.

### DATA AVAILABILITY STATEMENT

The data that support the findings of this study are openly available in [CASIA Dataset at [<http://biometrics.idealtest.org/>], reference number [PALMPRINT]. The data that support the findings of this study are openly available in [PolyU palm print database at [[https://www4.comp.polyu.edu.hk/~csajaykr/IITD/Database\\_Palm.htm](https://www4.comp.polyu.edu.hk/~csajaykr/IITD/Database_Palm.htm)], reference number [1.0].

### ORCID

Amjad Rehman  <https://orcid.org/0000-0002-3817-2655>

Majid Harouni  <https://orcid.org/0000-0003-0798-6100>

Tanzila Saba  <https://orcid.org/0000-0003-3138-3801>

## REFERENCES

- Ahmad, A. M., Sulong, G., Rehman, A., Alkawaz, M. H., & Saba, T. (2014). Data Hiding Based on Improved Exploiting Modification Direction Method and Huffman Coding. *Journal of Intelligent Systems*, 23(4), 451–459. <https://doi.org/10.1515/jisys-2014-0007>
- Almaghtuf, J., & Khelifi, F. (2018). Self-geometric relationship filter for efficient SIFT key-points matching in full and partial palm print recognition. *IET Biometrics*, 7(4), 296–304.
- Amin, J., Sharif, M., Raza, M., Saba, T., & Anjum, M. A. (2019). Brain tumor detection using statistical and machine learning method. *Computer Methods and Programs in Biomedicine*, 177, 69–79.
- CASIA Dataset. <http://biometrics.idealtest.org/>
- El-Tarhouni, W., Boubchir, L., Elbendak, M., & Bouridane, A. (2019). Multi-spectral palm print recognition using Pascal coefficients-based LBP and PHOG descriptors with random sampling. *Neural Computing and Applications*, 31(2), 593–603.
- Fahad, H. M., Khan, M. U. G., Saba, T., Rehman, A., & Iqbal, S. (2018). Microscopic abnormality classification of cardiac murmurs using ANFIS and HMM. *Microscopy Research and Technique*, 81(5), 449–457. <https://doi.org/10.1002/jemt.22998>
- Fei, L., Xu, Y., Teng, S., Zhang, W., Tang, W. & Fang, X. (2017). Local orientation binary pattern with use for palm print recognition. Paper presented at the Chinese conference on biometric recognition, 213–220.
- Harouni, M., Rahim, M. S. M., Al-Rodhaan, M., Saba, T., Rehman, A., & Al-Dhelaan, A. (2014). Online Persian/Arabic script classification without contextual information. *The Imaging Science Journal*, 62(8), 437–448. <https://doi.org/10.1179/1743131X14Y.0000000083>
- Iftikhar, S., Fatima, K., Rehman, A., Almazayad, A. S., & Saba, T. (2017). An evolution based hybrid approach for heart diseases classification and associated risk factors identification. *Biomedical Research*, 28(8), 3451–13455.
- Iqbal, S., Khan, M. U. G., Saba, T., Mehmood, Z., Javaid, N., Rehman, A., & Abbasi, R. (2019). Deep learning model integrating features and novel classifiers fusion for brain tumor segmentation. *Microsc Res Tech*, 82(8), 1302–1315. <https://doi.org/10.1002/jemt.23281>
- Jabeen, S., Mehmood, Z., Mahmood, T., Saba, T., Rehman, A., & Mahmood, M. T. (2018). An effective content-based image retrieval technique for image visuals representation based on the bag-of-visual-words model. *PLoS One*, 13(4), e0194526.
- Jadooki, S., Mohamad, D., Saba, T., Almazayad, A. S., & Rehman, A. (2017). Fused features mining for depth-based hand gesture recognition to classify blind human communication. *Neural Computing and Applications*, 28(11), 3285–3294. <https://doi.org/10.1007/s00521-016-2244-5>
- Jamal, A., Hazim Alkawaz, M., Rehman, A., & Saba, T. (2017). Retinal imaging analysis based on vessel detection. *Microsc Res Tech*, 80(7), 799–811. <https://doi.org/10.1002/jemt.22867>
- Joudaki, S., Mohamad, D. B., Saba, T., Rehman, A., Al-Rodhaan, M., & Al-Dhelaan, A. (2014). Vision-based sign language classification: a directional review. *IETE Technical Review*, 31(5), 383–391.
- Khan, M. A., Javed, M. Y., Sharif, M., Saba, T., and Rehman, A. (2019). Multi-model deep neural network based features extraction and optimal selection approach for skin lesion classification. 2019 international conference on computer and information sciences (ICIS) (pp. 1–7). IEEE.
- Khan, M. A., Sharif, M., Akram, T., Raza, M., Saba, T., & Rehman, A. (2020). Hand-crafted and deep convolutional neural network features fusion and selection strategy: An application to intelligent human action recognition. *Applied Soft Computing*, 87, 105986. <https://doi.org/10.1016/j.asoc.2019.105986>
- Khan, A. R., Doosti, F., Karimi, M., Harouni, M., Tariq, U., Fati, S. M., & Ali Bahaj, S. (2021). Authentication through gender classification from iris images using support vector machine. *Microscopy research and technique*, 84(11), 2666–2676.



- Khan, S. A., Nazir, M., Khan, M. A., Saba, T., Javed, K., Rehman, A., ... Awais, M. (2019). Lungs nodule detection framework from computed tomography images using support vector machine. *Microscopy Research and Technique*, 82(8), 1256–1266.
- Kumar, A. (2008). Incorporating cohort information for reliable palm print authentication. *Paper presented at the 2008 Sixth Indian Conference on Computer Vision, Graphics and Image Processing*, pp. 583–590.
- Kumar, A., & Shekhar, S. (2010). Personal identification using multi-biometrics rank-level fusion. *IEEE Transactions on Systems, Man, and Cybernetics, Part C (Applications and Reviews)*, 41(5), 743–752.
- Liu, L., Lao, S., Fieguth, P. W., Guo, Y., Wang, X., & Pietikäinen, M. (2016). Median robust extended local binary pattern for texture classification. *IEEE Transactions on Image Processing*, 25(3), 1368–1381.
- Liu, L., Zhao, L., Long, Y., Kuang, G., & Fieguth, P. (2012). Extended local binary patterns for texture classification. *Image and Vision Computing*, 30(2), 86–99.
- Lung, J. W. J., Salam, M. S. H., Rehman, A., Rahim, M. S. M., & Saba, T. (2014). Fuzzy phoneme classification using multi-speaker vocal tract length normalization. *IETE Technical Review*, 31(2), 128–136. <https://doi.org/10.1080/02564602.2014.892669>
- Meethongjan, K., Dzulkifli, M., Rehman, A., Altameem, A., & Saba, T. (2013). An intelligent fused approach for face recognition. *Journal of Intelligent Systems*, 22(2), 197–212.
- Minaee, S., & Wang, Y. (2016). Palm print recognition using deep scattering convolutional network. *arXiv preprint*, arXiv:1603.09027.
- Mittal, A., Kumar, D., Mittal, M., Saba, T., Abunadi, I., Rehman, A., & Roy, S. (2020). Detecting Pneumonia Using Convolutions and Dynamic Capsule Routing for Chest X-ray Images. *Sensors*, 20(4), 1068.
- Mokni, R., Drira, H., & Kherallah, M. (2017). Combining shape analysis and texture pattern for palmprint identification. *Multimedia Tools and Applications*, 76(22), 23981–24008.
- Neamah, K., Mohamad, D., Saba, T., & Rehman, A. (2014). Discriminative features mining for offline handwritten signature verification, 3D. *Research*, 5(2), 1–6. <https://doi.org/10.1007/s13319-013-0002-3>
- Nodehi, A., Sulong, G., Al-Rodhaan, M., Al-Dhelaan, A., Rehman, A., & Saba, T. (2014). Intelligent fuzzy approach for fast fractal image compression. *Biomedical Research*, 2014(1), 1–9.
- Ramzan, F., Khan, M. U. G., Rehmat, A., Iqbal, S., Saba, T., Rehman, A., & Mehmood, Z. (2020). A Deep Learning Approach for Automated Diagnosis and Multi-Class Classification of Alzheimer's Disease Stages Using Resting-State fMRI and Residual Neural Networks. *Journal of Medical Systems*, 44(2), 1–16.
- Rashid, M., Khan, M. A., Alhaisoni, M., Wang, S. H., Naqvi, S. R., Rehman, A., & Saba, T. (2020). A sustainable deep learning framework for object recognition using multi-layers deep features fusion and selection. *Sustainability*, 12(12), 5037.
- Raza, M., Sharif, M., Yasmin, M., Khan, M. A., Saba, T., & Fernandes, S. L. (2018). Appearance based pedestrians' gender recognition by employing stacked auto encoders in deep learning. *Future Generation Computer Systems*, 88, 28–39.
- Rehman, A., Alqahtani, S., Altameem, A., & Saba, T. (2014). Virtual machine security challenges: case studies. *International Journal of Machine Learning and Cybernetics*, 5(5), 729–742.
- Rehman, A., Khan, M. A., Mehmood, Z., Saba, T., Sardaraz, M., & Rashid, M. (2020). Microscopic melanoma detection and classification: A framework of pixel-based fusion and multilevel features reduction. *Microscopy Research and Technique*, 83(4), 410–423. <https://doi.org/10.1002/jemt.23429>
- Rehman, A., Khan, M. A., Saba, T., Mehmood, Z., Tariq, U., & Aysha, N. (2021). Microscopic brain tumor detection and classification using 3D CNN and feature selection architecture. *Microscopy Research and Technique*, 84(1), 133–149. <https://doi.org/10.1002/jemt.23597>
- Rehman, A., & Saba, T. (2011). Performance analysis of character segmentation approach for cursive script recognition on benchmark database. *Digital Signal Processing*, 21(3), 486–490. <https://doi.org/10.1016/j.dsp.2011.01.016>
- Rida, I., Heralut, R., Marcialis, G. L., & Gasso, G. (2019). Palm print recognition with an efficient data driven ensemble classifier. *Pattern Recognition Letters*, 126, 21–30.
- Saba, T. (2020). Recent advancement in cancer detection using machine learning: Systematic survey of decades, comparisons and challenges. *Journal of Infection and Public Health*, 13(9), 1274–1289.
- Saba, T., Haseeb, K., Ahmed, I., & Rehman, A. (2020). Secure and energy-efficient framework using Internet of Medical Things for e-healthcare. *Journal of Infection and Public Health*, 13(10), 1567–1575.
- Saba, T., Rehman, A., Al-Dhelaan, A., & Al-Rodhaan, M. (2014a). Evaluation of current documents image denoising techniques: a comparative study. *Applied Artificial Intelligence*, 28(9), 879–887.
- Saba, T., Rehman, A., Altameem, A., & Uddin, M. (2014b). Annotated comparisons of proposed preprocessing techniques for script recognition. *Neural Computing and Applications*, 25(6), 1337–1347. <https://doi.org/10.1007/s00521-014-1618-9>
- Saba, T., Rehman, A., Mehmood, Z., Kolivand, H., & Sharif, M. (2018). Image enhancement and segmentation techniques for detection of knee joint diseases: A survey. *Current Medical Imaging*, 14(5), 704–715.
- Sharif, U., Mehmood, Z., Mahmood, T., Javid, M. A., Rehman, A., & Saba, T. (2019). Scene analysis and search using local features and support vector machine for effective content-based image retrieval. *Artificial Intelligence Review*, 52(2), 901–925.
- Tamrakar, D., & Khanna, P. (2016). Noise and rotation invariant RDF descriptor for palmprint identification. *Multimedia Tools and Applications*, 75(10), 5777–5794.
- Xu, Y., Fei, L., & Zhang, D. (2014). Combining left and right palm print images for more accurate personal identification. *IEEE Transactions on Image Processing*, 24(2), 549–559.
- Yousuf, M., Mehmood, Z., Habib, H. A., Mehmood, T., Saba, T., Rehman, A., & Rashid, M. (2018). A Novel Technique Based on Visual Words Fusion Analysis of Sparse Features for Effective Content-Based Image Retrieval. *Mathematical Problems in Engineering*, 2018, 2134395. <https://doi.org/10.1155/2018/2134395>
- Zhang, S., Wang, H., Huang, W., & Zhang, C. (2018). Combining modified LBP and weighted SRC for palm print recognition. *Signal, Image and Video Processing*, 12(6), 1035–1042.

**How to cite this article:** Rehman, A., Harouni, M., Karchegani, N. H. S., Saba, T., Bahaj, S. A., & Roy, S. (2022). Identity verification using palm print microscopic images based on median robust extended local binary pattern features and k-nearest neighbor classifier. *Microscopy Research and Technique*, 85(4), 1224–1237. <https://doi.org/10.1002/jemt.23989>